Geochemistry and paleosedimentology of iron sulfide-rich carbonaceous mudstones in drill core DDKS-010: a tidally resedimented estuarine mudflat origin for surficially Ni-Zn-Cu-Co –enriched Paleoproterozoic Talvivaara formation (2.1–2.0 Ga), Finland

Jaakko J. Laitala[1] and Raimo Lahtinen[2]

[1]Department of Geosciences and Geography, University of Helsinki, P.O. Box 64, Helsinki, FI-00014, Finland; [2]Geological Survey of Finland, P.O. Box 96, Espoo, FI-02151, Finland

Abstract

Abstract. The Paleoproterozoic metasedimentary Talvivaara fm (2.1–2.0 Ga) in Sotkamo, Finland, hosts one of the largest sulfidic nickel resources in Europe (2053 Mt ore; Ni 4.5 Mt, Zn 10.3 Mt). Globally, the Talvivaara ore deposit is the largest shale-hosted Ni–(Cu–PGE) sulfide mineralization in production. We report here the preliminary results of our ongoing studies, which contradict the current genetic model relating the polymetallic Ni-Zn-Cu-Co –enrichment of the Talvivaara fm "black shales" to hydrothermal activity in a stratified rift basin. Sedimentology and geochemistry of drill core DDKS-010 (476.40 m) from the Kolmisoppi orebody was studied in detail, also additional trace element and high-resolution isotopic data was obtained. The intersection from 476.40 m to ca. 390 m forms stratigraphically nearly continuous well preserved succession, allowing an integrated study that has not been previously viable. Our results indicate a synsedimentary, paleomarine hydrogenous metal-enrichment for the C-S-Fe –rich Talvivaara fm mudstones–siltstones, and we interpret that the TV fm sediments were mainly tidally resedimented into deeper water, proximal offshore environment from a nearby estuarine mudflat.

Talvivaara Ore Deposit – Europe’s Largest Ni-Project

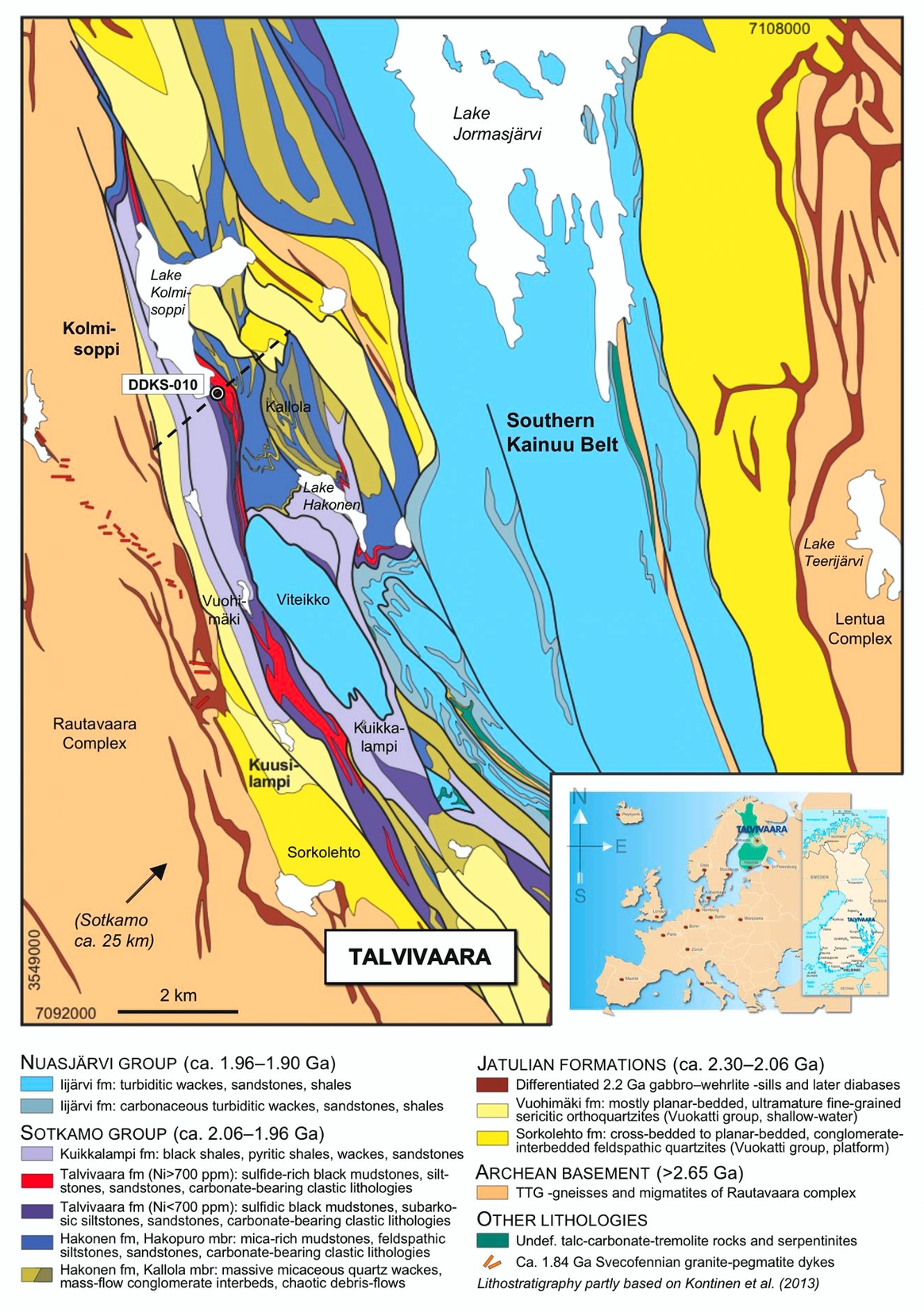
7108000
Lake Jormasjärvi
Kolmisoppi
Southern Kainui Belt
Lake Teerijärvi
Lentua Complex
Rautavaara Complex
(Sotkamo ca. 25 km)
TALVIVAARA
NUASJÄRVI GROUP (ca. 1.96–1.90 Ga)
Iijärvi fm: turbiditic wackes, sandstones, shales
Iijärvi fm: carbonaceous turbiditic wackes, sandstones, shales
SOTKAMO GROUP (ca. 2.06–1.96 Ga)
Kuikkalampi fm: black shales, pyritic shales, wackes, sandstones
Talvivaara fm (Ni>700 ppm): sulfide-rich black mudstones, siltstones, sandstones, carbonate-bearing clastic lithologies
Talvivaara fm (Ni<700 ppm): sulfidic black mudstones, subarkosic siltstones, sandstones, carbonate-bearing clastic lithologies
Hakonen fm, Hakopuro mbr: mica-rich mudstones, feldspathic siltstones, sandstones, carbonate-bearing clastic lithologies
Hakonen fm, Kallola mbr: massive micaceous quartz wackes, mass-flow conglomerate interbeds, chaotic debris-flows
JATULIAN FORMATIONS (ca. 2.30–2.06 Ga)
Differentiated 2.2 Ga gabbro–wehrlite -sills and later diabases
Vuohimäki fm: mostly planar-bedded, ultramature fine-grained sericitic orthoquartzites (Vuokatti group, shallow-water)
Sorkolehto fm: cross-bedded to planar-bedded, conglomerate-interbedded feldspathic quartzites (Vuokatti group, platform)
ARCHEAN BASEMENT (>2.65 Ga)
TTG -gneisses and migmatites of Rautavaara complex
OTHER LITHOLOGIES
Undef. talc-carbonate-tremolite rocks and serpentinites
Ca. 1.84 Ga Svecofennian granite-pegmatite dykes
Lithostratigraphy partly based on Kontinen et al. (2013)

FIG. 1. Geology of the Talvivaara area (map modified from Kontinen 2012). Sedimentary lithologies should be prefixed with ”meta”. Insert map: www.talvivaara.com

The deposit and mine. The Talvivaara ore deposit is located ca. 25 km from Sotkamo, eastern Finland (Fig. 1). The polymetallic Talvivaara ore deposit (Ni-Zn-Cu-Co-U) is comprised of Kuusilampi and Kolmisoppi orebodies, which together contain ca. 2053 Mt ore @ 4.5 Mt Ni and 10.3 Mt Zn (Talvivaara Plc. 2012, 2014), constituting one of the largest nickel resources in Europe (USGS 2013). The relatively low-grade but large tonnage sulfide ore is being utilized by using bacterially catalyzed bioheapleaching (Riekkola-Vanhanen 2013). Nickel deliveries started in 2009, and when in full-scale production, the mine is aiming at 50,000 t p.a. level (Talvivaara Plc. 2014). The Talvivaara ore deposit is currently genetically classified as SEDEX (Loukola-Ruskeeniemi and Heino 1996; Goodfellow and Lydon 2007), and as recently as 2014, Mudd and Jowitt (2014) included it in the category of hydrothermal Ni-deposits. Jowitt and Keays (2011, p. 194) review the hydrothermal genetic model proposed by Loukola-Ruskeeniemi and Heino (1996), but consider also the syngenetic, hydrogenous seawater scavenging model proposed by Kontinen et al. (2006). Globally, the metamorphically upgraded Talvivaara ore deposit is the largest shale-hosted Ni–(Cu–PGE) sulfide mineralization currently in production (Jowitt and Keays (2011).

Regional geology. The polymetallic Talvivaara ore deposit is hosted by the Paleoproterozoic C-S-Fe –rich Talvivaara formation, which belongs to the Sotkamo group (2.06–1.96 Ga) of primarily metasedimentary Kainuu Belt (Fig. 1.). Overview on the geology of the Kainuu Belt is provided by Laajoki (2005). The ca. 200-km-long Kainuu Belt overlies a reactivated Neoarchean suture zone between Archean blocks (Kontinen et al. 2007; Lentua and Rautavaara Complexes in Fig. 1.). Rifting of the Archean Karelian craton margin at 2.22–2.1 Ga and opening of Svecofennian paleosea at 2.1 Ga on the western side of the Rautavaara Complex led to extensional deepening of the Kainuu basin (Lahtinen et al. 2008; Korja et al. 2006). The initial block faulting phase included chaotic sedimentation in the lower Sotkamo group (Gehör and Havola 1988), and 2.1 Ga mafic tuffite interbeds in clastic shallow-water carbonates at Melalahti, Paltamo (60 km NNW of Talvivaara), indicates local magmatism during the incipient rifting stage (Kärki 1988). Epiclastic, compositionally Fe-tholeiitic amphibolite schist interbeds occur also in silicate-facies iron formation units of Tuomivaara and Tenetti formations (ca. 30 km NNE of Talvivaara), which belong lithostratigraphically to the lower or middle part of the Sotkamo group (Gehör and Havola 1988).

The Paleoproterozoic evolution of supracrustal sequences in nearby Russian Karelia is recently synthesized by Melezhik et al. (2013), and the chronostratigraphic division by Hanski and Melezhik (2013) for the Fennoscandian Shield is adopted here. Lower age for the Sotkamo group can be defined by the end of the Jatulian system (2.30–2.06 Ga) that includes the GOE (Great Oxygenation Event) and the related global Lomagundi–Jatuli $\delta^{13}C$ -isotopic excursion recorded by sedimentary carbonates (Karhu 1993; Karhu and Holland 1996). Termination of the Jatulian system is precisely bracketed at 2.058–2.060 Ga (Hanski and Melezhik 2013). The Sotkamo group belongs in a chronostratigraphic sense to the Ludicovian system (2.06–1.96 Ga) of Hanski and Melezhik, which is traditionally in Finland referred in lithostratigraphical sense as Lower Kaleva. As the Ludicovian of Russian Karelia include the type locality for the global Shunga -event (worldwide deposition of significantly C_{org}-rich sediments; Melezhik et al. 2013, p. 1195–1273), we adopt the Ludicovian system also for Finnish usage. The Talvivaara formation is thus regionally correlated here with the C_{org} -rich sedimentary rocks of the 2.05–1.98 Ga Zaonega fm in the Russian Karelia (op. cit.), and globally e.g. with the 2.08–2.02 Ga black shales of the Francevillian basin, Gabon (Ossa Ossa et al. 2013).

Lithostratigraphy and metamorphism in the Talvivaara area. Kontinen et al. (2013) have recently described the main lithostratigraphic units[1] in the Talvivaara area, which are summarized in Fig. 1. The C_{org} and sulfide-rich black mudstone–siltstone dominated metalliferous Talvivaara formation (TV fm) is underlain by the micaceous sandstone–siltstone dominated Hakonen fm (HK fm), and Kontinen et al. (2013) view the transition as abruptly gradational. The relation to the non-metal enriched overlying Kuikkalampi fm (KL fm) is similarly considered as abruptly gradational, although yet inconclusively defined. As a departure from Kontinen et al. (2013), the Nuasjärvi group (1.96–1.90 Ga) is here taken to represent autochtonous–parautochtonous deep-water sedimentary units (Gehör and Havola 1988) that were back-thrusted in structural inversion and tectonic stacking of the closing intracratonic marginal basin during the 1.90–1.87 Ga Svecofennian orogeny (Korja et al. 2006; Lahtinen et al. 2008). Metamorphic peak at 1.88–1.87 Ga is given by U–Pb -ages from Talvivaara uraninites (Lecomte et al. 2014). Although regional metamorphism in the Kainuu Belt ranges from amphibolite facies in the west to lower greenschist facies in the east (Laajoki 2005), geobarometry by Törnroos (1982) indicates possible low-pressure domains at Kolmisoppi.

Prevailing hydrothermal ore-genetic model – and recent advances. Since the genetic synthesis paper by Loukola-Ruskeeniemi and Heino (1996), the Talvivaara fm sediments have been mostly referred as hydrothermally Ni-Cu-Zn -enriched S and C_{org} -rich black shales (*sensu lato*) deposited in the deeper part of a stratified, restricted marine rift basin (e.g. Pasava et al. 2003; Jowitt and Keays 2011). High median C_{org} (7.6 wt %) and S (8.2 wt.%) -values attest for anoxic/euxinic conditions, and iron sulfide $\delta^{34}S$ -data have been interpreted as evidencing for both bacterial and thermochemical SO_4 -reduction (Loukola-Ruskeeniemi and Lahtinen 2013). Recently, Young et al. (2013) have also used anomalous fractionations in $\delta^{33}S$ -data and $\Delta^{33}S$ -values as arguing for thermochemical reactions during interactions of sulfate-rich hydrothermal fluids with the Talvivaara muds. Ultramafic rocks (serpentinites) occurring in the area have been considered as the most plausible source for Ni (Loukola-Ruskeeniemi et al. 2013). However, recent studies by Kontinen (2012) have placed tight geological constraints for the hydrothermal model: base-metal and trace-element ratios in Talvivaara point towards redox-controlled synsedimentary metal-enrichment in a well-connected marine basin with temporally anomalous seawater Ni, Zn, Cu and Co concentrations. Compositional homogeneity of individual mud beds, varying metal concentrations between adjoining sedimentation units (laminae, beds), and mass-flow features have indicated possible re-depositional origin for the metalliferous muds (Kontinen et al. 2013). Similar average metal concentrations in other ca. 20 smaller Talvivaara-type occurrences in eastern Finland also support larger basinal controls (Rasilainen et al. 2013, p. 15–17). Other recent studies of Talvivaara are provided by Törmälehto (2008), Laitala (2014a,b), and Virtasalo et al. (2014).

---

[1] This nomenclature should be understood as ”work in progress”, as the formal status of the Talvivaara fm (and other local units belonging to the Sotkamo group) is currently undefined in the national bedrock database of Finland (FinStrati, DigiKP200; www.gtk.fi). The nomenclature of Kontinen et al. (2013) is presently used here in informal sense.

Kolmisoppi Drill Core DDKS-010: Obtaining the Material

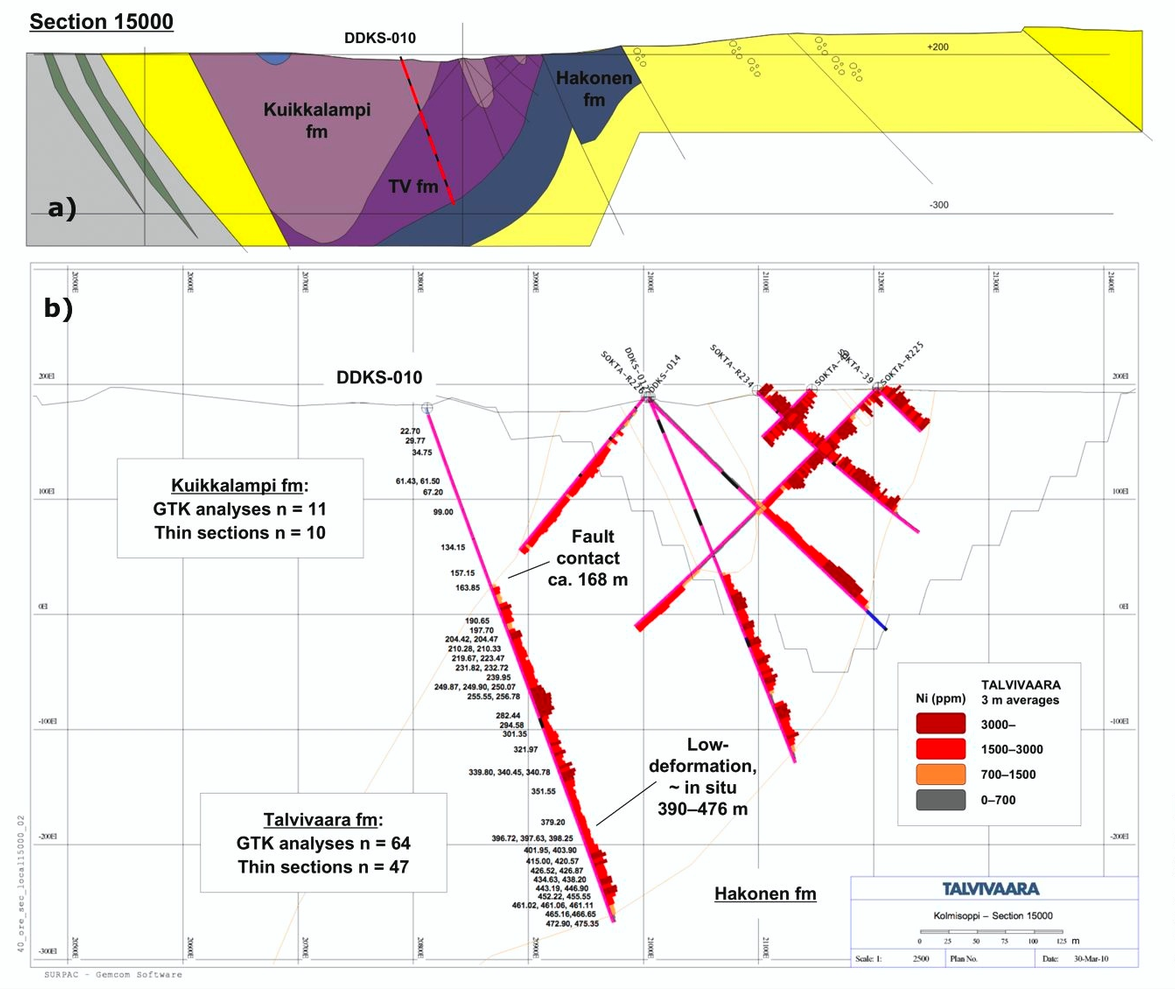

Selecting DDKS-010. After completion of a prioritized campaign at the newly opened Kuusilampi open pit, resource definition drilling programme by Talvivaara Plc. (2010) began delineating the dimensions of Kolmisoppi orebody more precisely in 2009. As some of the fresh Kolmisoppi cores showed excellent partial preservation of the TV fm sedimentary lithologies, they were sampled by GTK geologist Asko Kontinen in 2009. These initial results led to launching the present project in January 2010. Final selection of the core suitable for detailed study was done by (then) Talvivaara Plc. mining geologist Hannu Lahtinen and A. Kontinen. Despite tight overfolding (Fig. 2.) and partial tectonic repetition of lithological units, DDKS-010 preserves the lower parts of TV fm relatively intact up to circa 390 m. Only very basic structural analysis was undertaken in this study.

Drill core logging and sampling (GTK). Drill core DDKS-010 was logged, studied and sampled at the Talvivaara core facility in 2010. The core was digitally photographed (Canon PS G9, RAW image format; 3 hi-res pictures per box + close-ups), measured, and sampled for whole-rock chemical analyses (n=75) and thin sections (n=57).

FIG. 2. a) Geological section of DDKS-010 showing lithological units of the Kolmisoppi drilling profile 15000 (see Fig. 1.). Modified from picture drawn by Asko Kontinen. **b)** SURPAC -section by Talvivaara Mining Co. displaying 3-m average Ni-concentrations in drilling holes at Kolmisoppi orebody, section 15000 (as in year 2010). Depths of GTK thin section samples (not resolvable here) are marked on the left side of the DDKS-010 column. TVA Plc. cut-off limit for chemical analyses is 700 ppm Ni. Scale bar: 125 m.

Talvivaara Plc., DDKS-010 Average Data (164–476 m)

DDKS-010, Chemical average data by Talvivaara Plc. As an integral part of mineral resource inventorying, deposition-scale modeling, and delineating the Kuusilampi and Kolmisoppi orebodies, Talvivaara Mininc Co. Plc. performs chemical whole-rock analyses for longer drill core intersections displaying >700 ppm Ni (cut-off limit for mining) in hand-held XRF. TVA Plc. uses 3-meter sample length for averaging, and the analyzed sections are sampled continuously (further methods used by TVA Plc. can be found in Loukola-Ruskeeniemi and Lahtinen 2013). At the initiation of this GTK study, TVA Plc. mining geologist Hannu Lahtinen provided the present authors with chemical average data from the analyzed intersection of Kolmisoppi drill core DDKS-010 (164–476 m; Fig. 2.). Some of the whole-core average data is visualized in Figs. 3. and 4. The TVA Plc. average data was used in pre-planning and targeting the detailed GTK sampling.

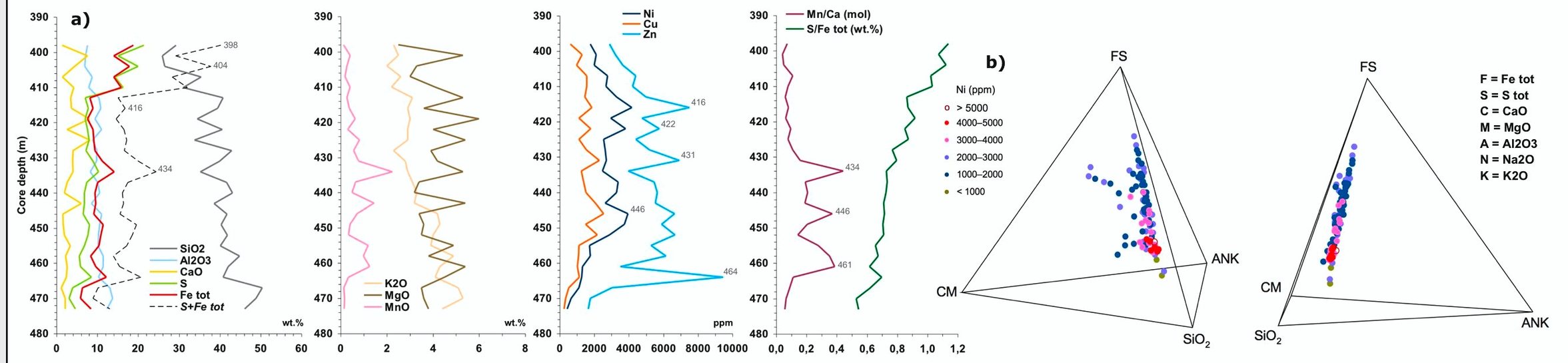

FIG. 3. a) Simple profile diagrams between depths 398–476 m showing selected main and minor element average concentrations and ratios in drill core DDKS-010 (sample length 3 m, data by Talvivaara Plc.). **b)** Main element molar ratio diagram for all TVA Plc. 3-m average analyses (n=104) between depths 164–476 m in DDKS-010. Average Ni levels are shown with colour codes (Note: colours in Ni legend are not to be confused with Fig. 3.a).

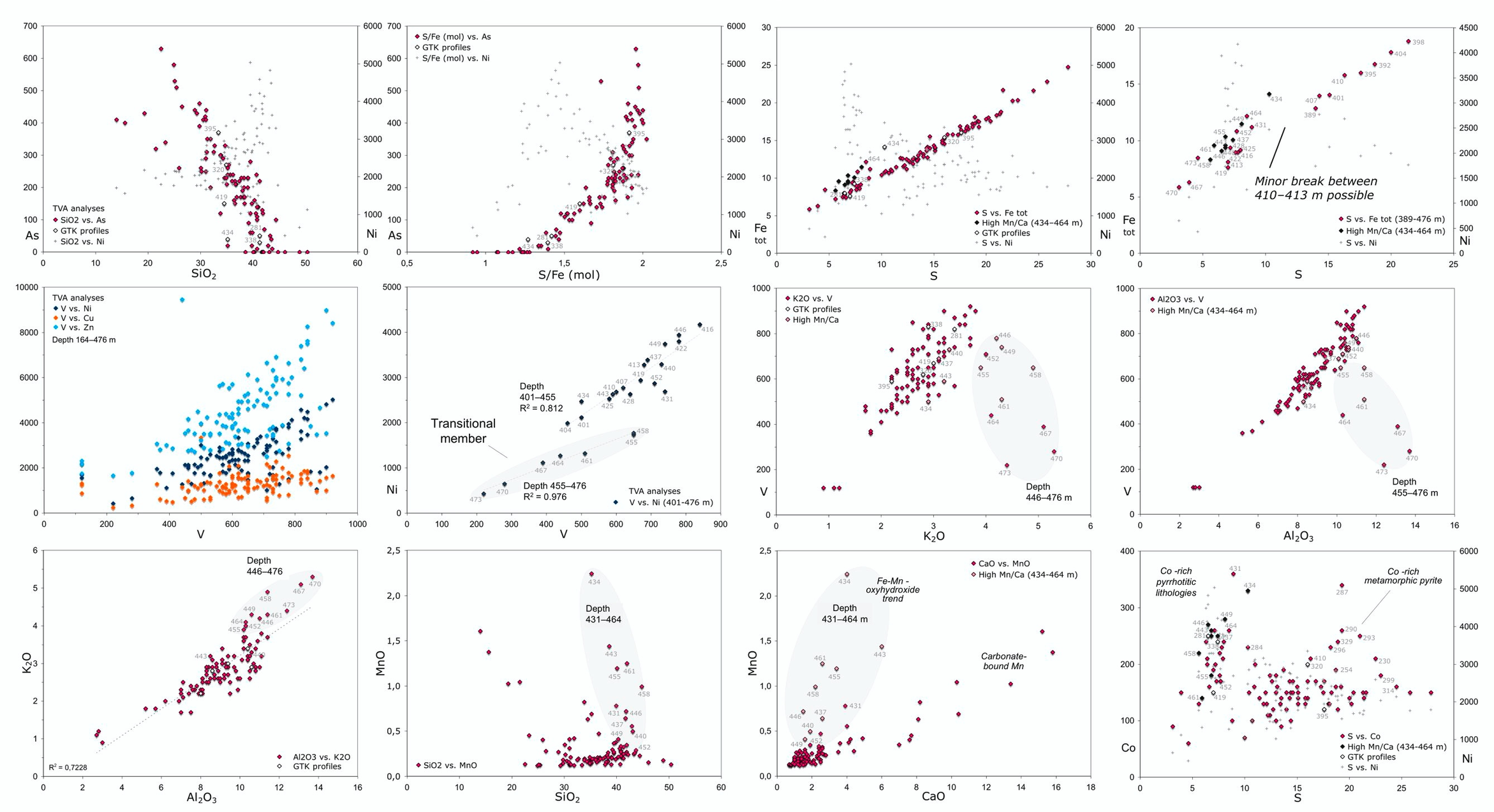

FIG. 4. Binary (and trinary) plots from the TVA Plc. average data in DDKS-010 (sample length 3 m, depths 164–476 m, n=104). Depths of GTK profiles are indicated. **Top row:** Diagrams showing variations in the amounts of pyrrhotite and pyrite. As is a good proxy for syngenetic pyrite. Lowering of average Ni -concentrations with increasing amount of pyrite is clear in *"S/Fe (mol) vs. As"* and *"S vs. Fe"* -diagrams. **Mid row:** Vanadium has good overall linear correlatios with Ni, Cu and Zn. Diagram *”V vs. Ni at depths 401–476 m”* suggests separate detrital mica-bound and clay-bound vanadium. Upper depth of "transitional siltstone mbr" of Talvivaara fm is positioned here at ca. 455 m based on *"V vs. Ni"*, *"K_2O vs. V"* and *"Al_2O_3 vs. V"* -diagrams. **Bottom row:** K-feldspathic sand–silt component in the "transitional siltstone mbr" can be seen in higher K/Al at depths 455–476 m, mica-bound K_2O is high at 455–446 m. *"SiO_2 vs. MnO"* and *"CaO vs. MnO"* -diagrams show that besides carbonate-bound MnO, there are clearly lithologies with non-carbonate bound Mn (currently in spessartine). High Mn/Ca (molar) -ratio is interpreted to indicate primary lithologies rich in Fe-Mn oxyhydroxides. *”S vs. Co”*: Cobalt has good correlation with Ni; also separate high-Co trend related to stronger deformation and secondary metamorphic pyrite is seen at drill core depths near the fold hinge zone (ca. 285–305 m).

GTK Samples and Results: Integrated Sedimentology, Petrography and Geochemistry

GTK sample materials and methods. Sampling for this study (Laitala 2014a) aimed at representative coverage of the whole drill core DDKS-010, although focusing on the metal-enriched TV fm (Fig. 2.). Lithologies from the KL fm were sampled for comparison. Total number of chemical samples was 75 (TV fm, n=64; KL fm, n=11), and number of polished thin sections was 57 (TV fm, n=47; KL fm, n=10). Sampling was targeted on visually well-preserved parts but some sections showing minor shearing, silicification and slight mobilization of sulfides were sampled for controlling secondary effects (Fig. 5.). Strongly sheared or obviously altered parts in DDKS-010 were avoided. Six chemical profiles were taken (indicated in figures as Profs. 1.–5.; Prof. 6. is grouped in ”Mn-rich pyrrhotite mudstones”), plus several additional sample pairs. Whole-rock chemical analyses were performed by Labtium Ltd., Espoo, using XRF and Leco (C_{carb}, C_{org}) -methods. Continuous, good-quality drill core box pictures served as sedimentological documentation (Fig. 6.). Additional mineralogical (SEM, EPMA) and high-resolution *in situ* iron sulfide Fe- and S -isotope data (NordSIM, Stockholm; results in preparation) were also obtained, and Virtasalo et al. (2014) performed a separate *in situ* $\delta^{34}S$- and $\delta^{56}Fe$ -study on laminated pyrite-rich samples at depth 406.15–406.55.

Petrographic studies and the present mineralogy of samples. DDKS-010 thin sections were optically scanned for macroscopic details, then microscoped at transmitted and reflected light (Fig. 6.). About thousand microphotographs were taken. Grain-scale isotopic heterogeneities in metaframboidal sedimentary pyrites indicate good preservation of primary signatures despite metamorphic recrystallization. Present main sulfides are pyrite (descriptively subdivided to Py_1–Py_5), pyrrhotite (Po_1–Po_5), sphalerite (Sph), pentlandite, chalcopyrite and alabandite; other mineral phases are quartz, K-feldspar (orthoclase to microcline), phlogopite, biotite, muscovite, plagioclase, carbonate (dolomite to calcite), tremolite, spessartine, rutile, titanite, apatite and thucholite (bitumen-rimmed uraninite grains), detrital zircon and monazite often display secondary xenotime overgrowths. Pyrite may be completely absent in some lithologies. Carbonaceous matter was petrographically broadly divided to kerogenous (inert restite), bitumenous (mobilated) and graphitic (optically anisotropic) substances.

Sample screening and classification. Inhibitory effect of high C_{org} -content on metamorphic recrystallization of Paleoproterozoic sulfidic black shales was already noted by Peltola (1960). Sulfide-rich black metashales (”black schists”) occur widely in Finland, and Kontinen et al. (2006) recognized the value of their more detailed lithofacies study. Samples in the present GTK study were screened to chemical alteration categories 1a, 1b, 2 and 3, based on combined elemental coherence, drill core preservation and thin section petrography (Figs. 5.–7.). Although Bekker et al. (2010) disregard the notion of sulfide-facies iron formation, many features observed in DDKS-010 are consistent with the definition of sulfide-facies iron formation *sensu* James (1966). Pyrite-dominated laminated lithofacies forms one sedimentary endmember in Talvivaara fm (Fig. 7a–b.), and Laajoki and Saikkonen (1977) have described laminated pyrrhotite-rich units in the broadly contemporary basin-margin iron formations of the Kainuu Belt. High iron-sulfide content and good preservation of the DDKS-010 samples necessitated treating syngenetic–early diagenetic pyrite grains as sedimentary component (e.g. Love and Zimmerman 1961), and a sedimentology-based, semi-quantitative geochemical–petrographical classification was developed for the sulfidic metasedimentary lithofacies applicable to the Talvivaara region (Laitala 2014a). Formation of marine sedimentary sulfides is reviewed by Rickard (2012), and it is both conceptually and paleoenvironmentally important to make a distinction to iron sulfide-rich sediments occurring in SEDEX -environments (as described e.g. in Lydon et al. 2000; Goodfellow and Lydon 2007).

Sedimentology. The present short discussion focuses on the stratigraphically nearly continuous well-preserved section of DDKS-010 between 476.40 m to 390 m. Illustrations are found in Fig. 6., and the pictures are referred by core / thin section (TS) depths. Overall, the sequence is interpreted as a transgressive, gradational transition from the underlying HK fm to the metal-rich TV fm. Talvivaara fm is divided here informally into transitional pyrrhotitic siltstone member (ca. 476.40–455 m), pyrrhotitic mudstone member (455–431 m), and pyritiferous mudstone member (431–390 m). The clastic sedimentary terminology used here broadly follows Potter et al. (2005).

The transitional siltstone mbr of TV fm is dominated by subarkosic, partly very biotite-rich, muddy siltstones–fine sandstones and...

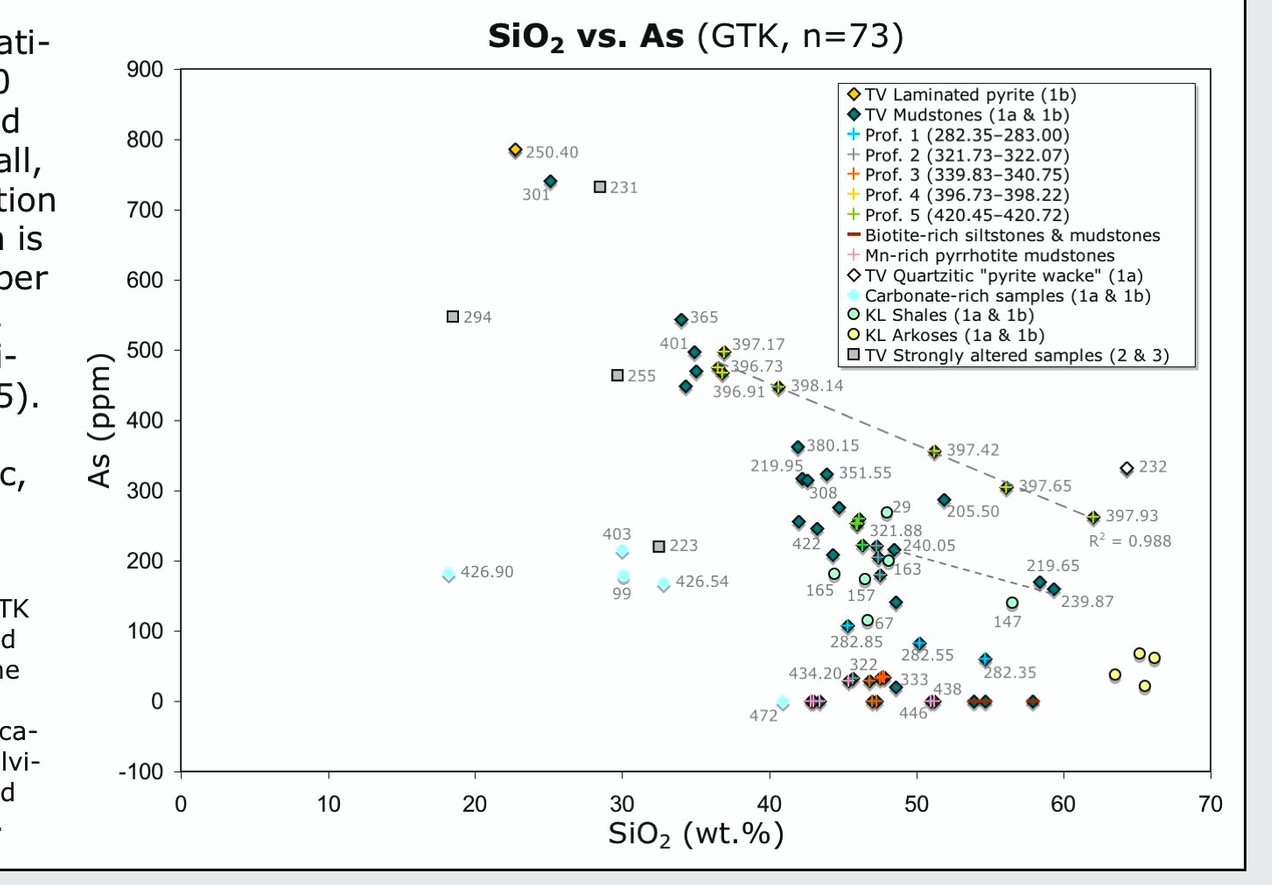

FIG. 5. SiO_2 vs. As -diagram was utilized as a part of the screening procedure for GTK samples, which were designated to alteration categories 1a, 1b, 2 and 3. As is a good proxy for syngenetic–diagenetic pyrite, and sheared 1b samples mainly show only the volumetric dilution by metamorphic silica. Non-altered Cat 1a samples were further used as a basis for more detailed, semi-quantitative chemical–petrographical classification of the sulfidic mudstones, siltstones and shales (claystones) belonging to the Talvivaara and Kuikkalampi formations. The full classification scheme, primarily developed for sulfidic sedimentary rocks in the Talvivaara region, is included in Laitala (2014a).

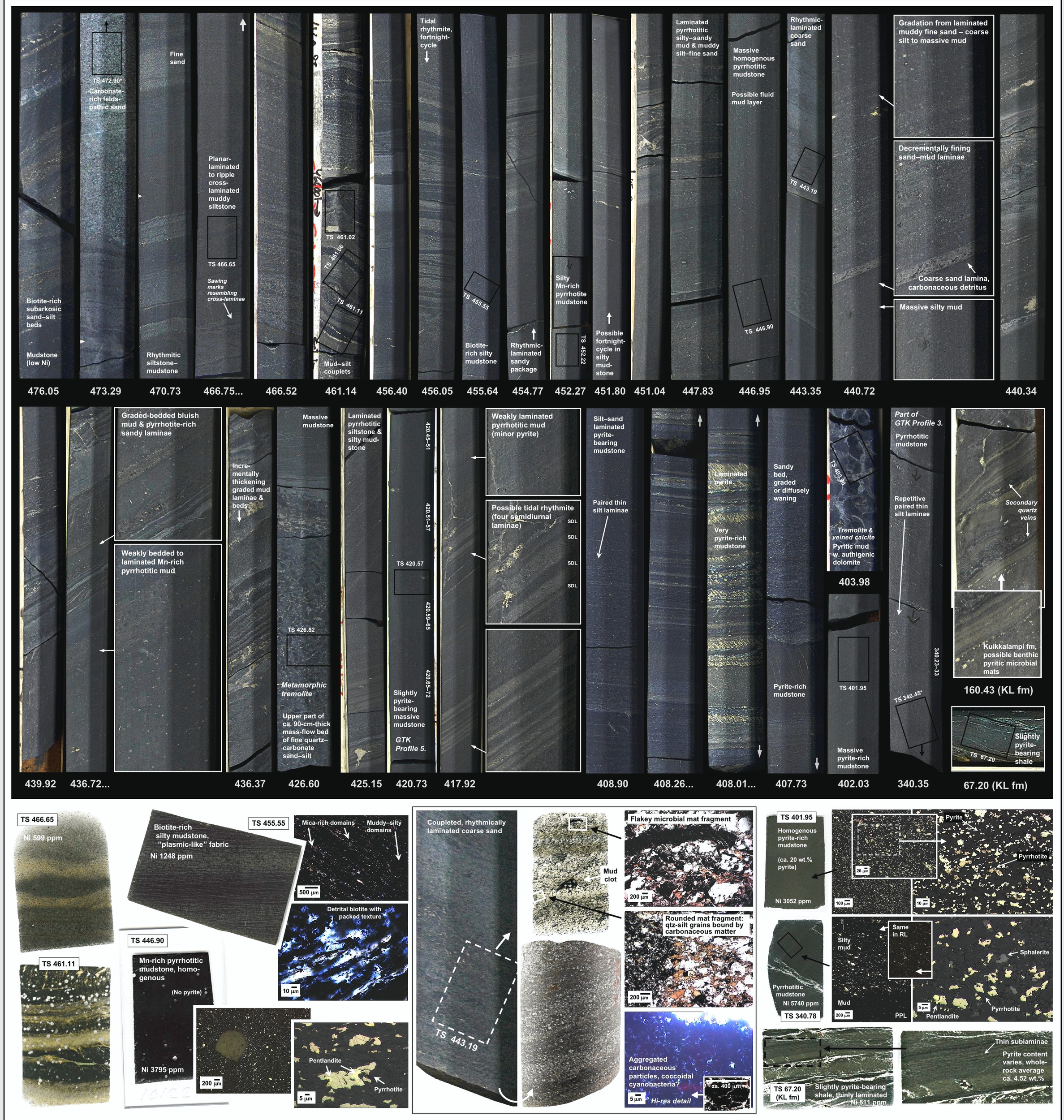

FIG. 6. Drill core pictures: Representative lithologies in the stratigraphically nearly continuous, well-preserved lower part of DDKS-010. Talvivaara fm is divided here informally to "transitional pyrrhotitic siltstone member" (ca. 476.40–455 m), "pyrrhotitic mudstone member" (455–431 m) and "pyritiferous mudstone member" (431–390 m). Picture 340.35 shows part of the GTK profile 3., which has the highest systematic Ni-trends of the studied samples. Drill core pictures of Kuikkalampi fm pyritic shales (claystones) and slightly pyritic black shales (*sensu stricto*) are shown at lower right. Scale of the pictures varies, but core diameter is 4 cm. Part of the core box is shown for colour/brightness reference in some images. Approximate positions of GTK thin section samples are also marked. Note: drill core depths here are only close estimates serving as image identifiers, not precise measured depths. **Thin section pictures:** A few examples of thin sections examined in the present study (Laitala 2014a), see the poster text for more explanations.

Sedimentology (continues). ...low-Ni black mudstones showing initially graded bedding (476.05; 473.29), but transitioning quickly to rhythmic sedimentation displaying diagnostic features of depositional environment with semidiurnal tidal cyclicities (e.g. Williams 2000; Kvale 2012). Thinly mud-draped, horizontally laminated gray silts–fine sands in 470.73 form rhythmically alternating packages with laminated dark silt-rich muds, apparently recording daily to semi-monthly or monthly tidal periodicities as detailed by Adkins and Eriksson (1998). Small-scale ripple cross-lamination in TS 466.65 attests also for intermittent dynamic migratory bedform sedimentation of the muddy silts, either from turbidites (Schieber 1990) or waning tidal currents (Jaeger and Nittrouer 1995). Abruptly erosive contact and decrementally fining laminae (from coarse sand to muddy fine sand–silt) in 466.52 may relate to successively weakening ebb-tide current velocities (De Boer et al. 1989). Heterolithic, rhythmically interlaminated graded mica-rich silt/black mud -couplets in 461.14 (TS 461.11) are a classic feature of vertically accreted tidal rhythmites (Cowan et al. 1998). At 456.05, systematic thickness variations in heterolithic sand–silt/mud -couplets seem to record a symmetric, full fortnight cycle (neap–spring–neap): about 28 semidiurnal lamina couplets (ordinate and subordinate lamina couplets) can be counted, which would indicate the deposition of 20-cm-thick sequence in ca. 14 days (Adkins and Eriksson 1998, Fig. 6.; Smith et al. 1990). Upper part of the transitional siltstone member of TV fm can be recognized as increasing dominance of black silty mudstones (455.64; see also Fig. 4.), and TS 455.55 appears to retain a plasmic microfabric (Kuehl et al. 1988; Allison et al. 1995) in horizontally aligned (S_0/S_1) detrital biotite flakes occurring as unistrially concentrated layers.

The pyrrhotitic mudstone member of TV fm (454.77 to 436.37) is dominated by black, fine, clay-rich mudstones having higher sapropelic C_{org} -component and significantly elevated metal concentrations. Frequently occurring rhythmic-laminated sandy packages (e.g. 454.77, 451.04, 443.35, 440.34, 439.92) continue interluding the mud deposition repeatedly (recurring intervals vary from decimeters to metres), apparently recording periodicities from monthly to annual to pluriannual lunar cycles, and seasonal changes in paleotidal range (Williams 2000). In many cases, the sandy packages display similar overall tripartite rhythmicity as in the lower part of image 470.73. Depositional fabrics of the TV fm pyrrhotitic mudstones are illustrated in the core pictures, but completely featureless homogenous thick mud layers (as in 446.95) possibly represent deposition from mobilized fluid muds (Jaeger and Nittrouer 1988; Mackay and Dalrymple 2011). Carbonaceous detritus in interluding, rhytmically laminated coarse sand package in TS 443.19 has been interpreted as eroded from nearby...

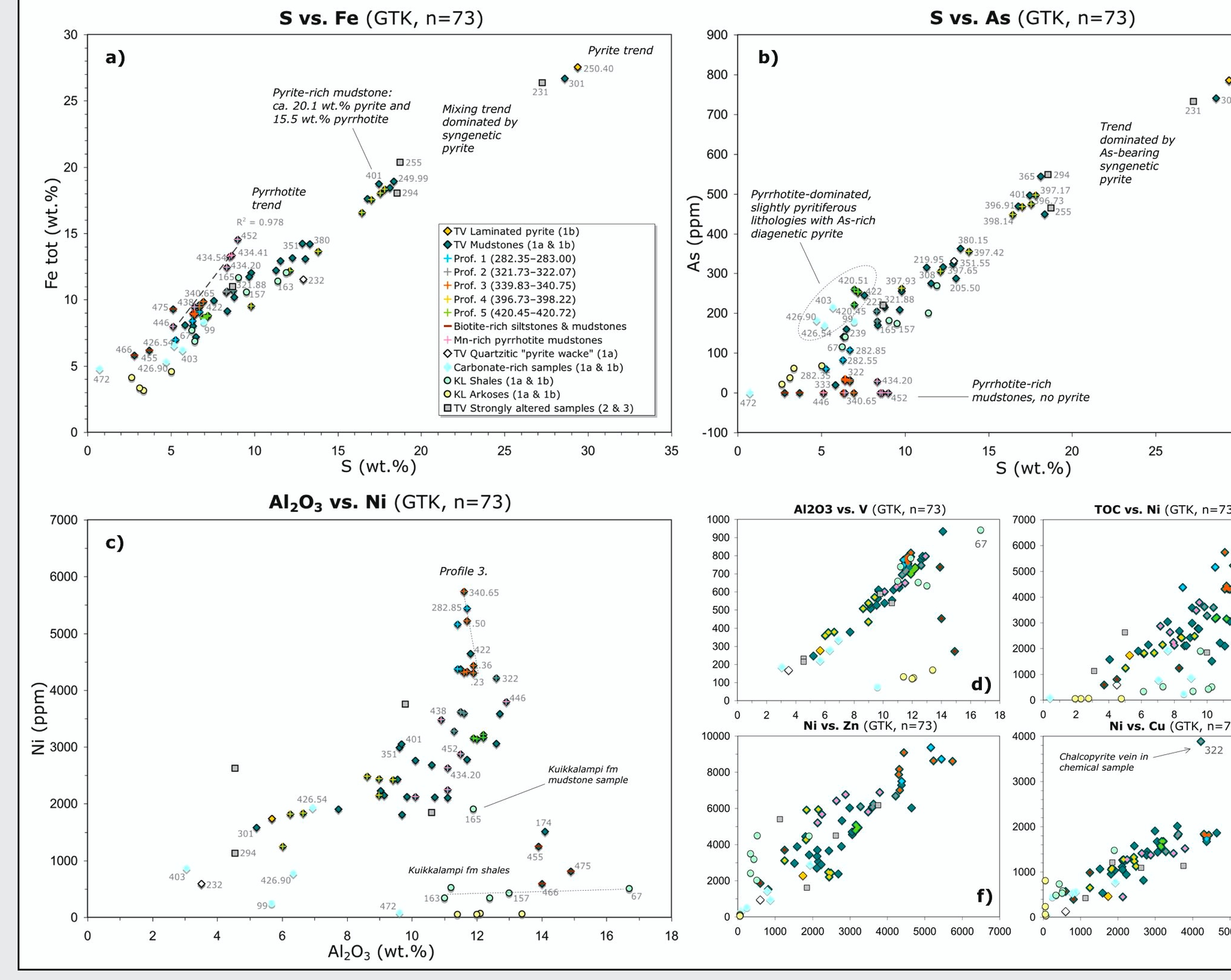

FIG. 7. a) *S vs. Fe $_{tot}$* of the GTK data shows the variation in iron sulfide components. We interpret the distinct separate pyrrhotite trend as representing a primary feature related to precursor sulfide(s) and abundant Fe-Mn oxyhydroxides in sediments, not as metamorphic pyrrhotitization of pyrite. **b)** *S vs. As* agrees well with thin section observations: high As/S -samples occur mostly at depths where minor diagenetic pyrite is first introduced in the sediments. **c)** *Al_2O_3 vs. Ni* shows good overall correlation of Ni with clay-bound Al_2O_3, which is further attributed to clay–C_{org} -association. **d–h)** Simplified diagrams showing some correlations of redox–sensitive elements in GTK data. Major elements are in (wt.%), minors in (ppm). Scatter in Zn/Ni may relate to ready mobilization of sphalerite in more permeable (siltier) mudstones, or primary microbial formation of additional sedimentary sphalerite.

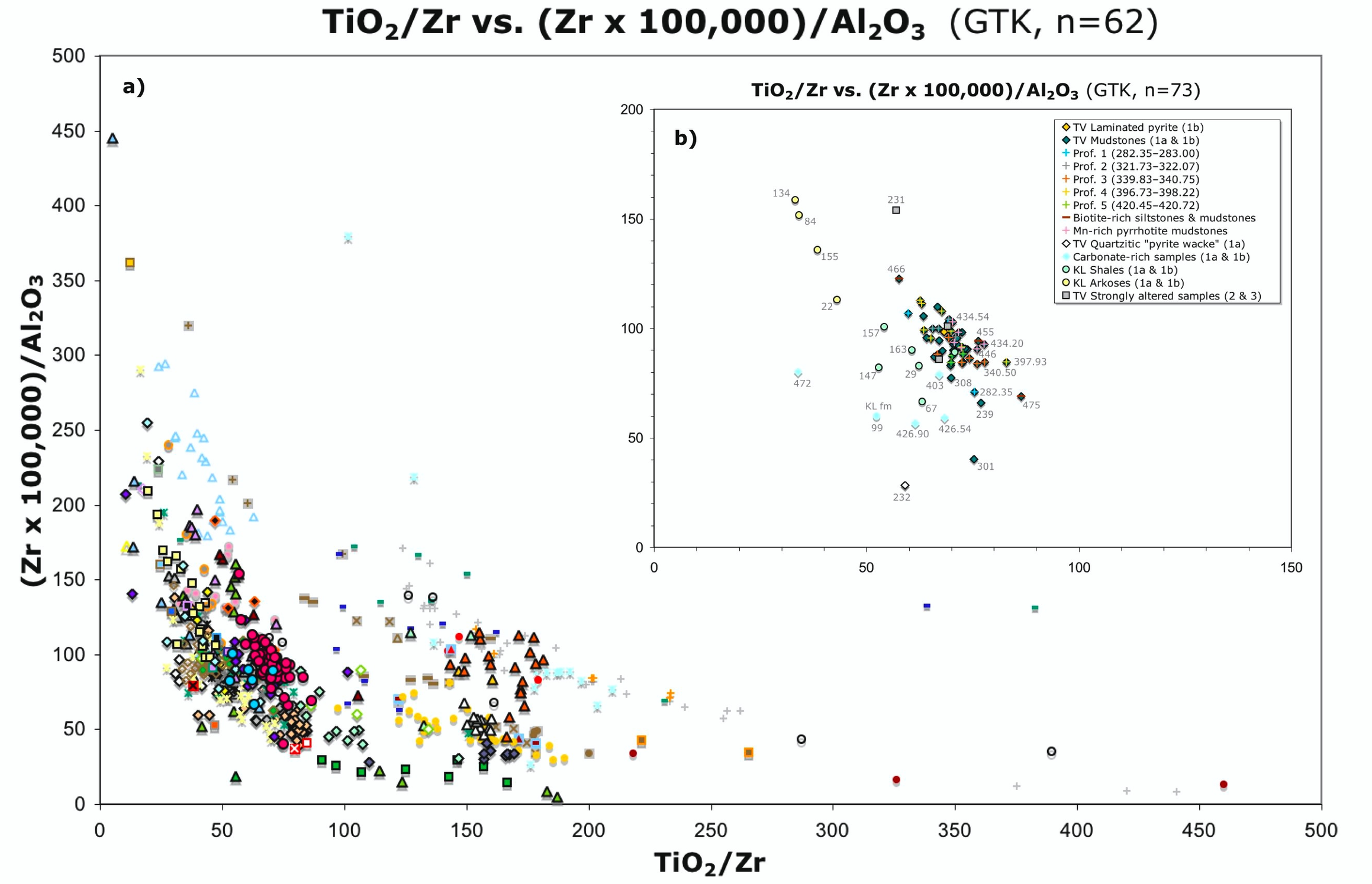

Talvivaara – Kolmisoppi DDKS-010, this study:

- ● DDKS-010, Talvivaara formation, all mudstones–siltstones [n=56]
- ● DDKS-010, Kuikkalampi formation, all shales–mudstones [n=6]

Note: carbonate-rich samples and sands have been omitted here.

Talvivaara – Samples in other studies:

- ☒ GTK all, median [n=100] (Loukola-Ruskeeniemi & H. Lahtinen 2013)
- ◇ GTK-350, all samples, Ni<700 ppm (L-R & HL 2013)
- ◆ GTK-329, all samples (L-R & HL 2013)
- ☒ TV Plc., waste samples [n=107] median (L-R & HL 2013)
- ☐ TV Plc., ore samples [n=556] median (L-R & HL 2013)
- ◆ TV Plc., cores TAL-188, 220, 238 & 233 (L-R & HL 2013)

Finnish reference metasedimentary rocks:

- ◇ Nurmes, 2.7 Ga paragneiss mesosomes (Kontinen et al. 2007)
- ◆ Nurmes, 2.7 Ga paragneiss mesosomes Cr > 300 (Kontinen et al. 2007)
- ◇ Petäjäskoski Fm, >2.14 Ga claystones–mudstones (Kyläkoski et al. 2012)
- ◆ Peräpohja, 2.1 Ga Martimo Fm black shales (Perttunen & Hanski 2003)
- ☐ Karelian & Svecofennian averages from Lahtinen 2000 (Tables 1. & 2.)
- ☐ Höytiäinen basin, H2-metasediment (high Cr) average (Lahtinen 2000)
- ☐ Outokumpu black schists & shales, median [n=2943] (Kontinen et al. 2006)
- ☐ Upper Kaleva, black schist average (Kontinen et al. 2006)

Global reference sedimentary rocks & shale averages:

- ✱ African Archean–Paleoproterozoic shales & mudstones (Siebert et al. 2005)
- ◇ Barberton, Fig Tree 3.24 Ga graywackes (Toulkeridis et al. 1999)
- ◆ Barberton, Moodies 3.2 Ga shales (Hessler & Lowe 2006)
- ◇ Barberton, Moodies 3.2 Ga sandstones (Hessler & Lowe 2006)
- △ Belingwe, Zeederbergs Fm 2.7 Ga shales (Hofmann et al. 2003)
- ◇ Belingwe, Cheshire Fm 2.7 Ga shales (Hofmann et al. 2003)
- ▲ Birimian Group, 2.1 Ga shales (Roddaz et al. 2007)
- ▲ Birimian Group, 2.1 Ga Fe-shales (Roddaz et al. 2007)
- △ Birimian Group, 2.1 Ga subarkose (Roddaz et al. 2007)
- ▲ Cuddapah Basin, <2.1 Ga black shales (Manikyamba et al. 2008)
- △ Gwalior Group, 1.9 Ga shales (Absar et al. 2009)
- ■ Sullivan, 1.47 Ga Aldridge Fm arenite average [n=15] (Lydon et al. 2000)
- ■ Sullivan, 1.47 Ga Aldridge Fm siltite average [n=58] (Lydon et al. 2000)
- ■ Sullivan, 1.47 Ga Aldridge Fm argillite average [n=27] (Lydon et al. 2000)
- ✱ Iberian Pyrite Belt, Rio Tinto district black mudrocks (Boulter et al. 2004)
- ✱ Paja Fm, Lower Cretaceous black shales (Campos Alvarez & Roser 2007)
- ◇ Sukhoi Log, Khomolko Fm pyritic black shale (Large et al. 2011)
- ■ Bazhenov Fm, average [n=30 drill cores] (Gavshin & Zakharov 1996)
- ✱ Brumsack (2006), Table 2a. reference lithologies & averages
- ■ WGA – Worldwide graywacke average (Wedepohl 1995)
- ■ PAAS – Post Archean Average Shale (Taylor & McLennan 1985)
- ■ ANABS – Average North American Black Shale (Vine & Tourtelot 1970)
- ☐ SDO-1 Black shale average (Huyck 1989)

Fennoscandian mafic–ultramafic igneous rocks & pyroclastics:

- ■ Peräpohja Belt, 2.2-2.1 Ga mafics (Perttunen & Hanski 2003):
  - ● - Tikanmaa tuffites
  - + - Hirsimaa tuffites
  - △ - Lamulehto tuffite
  - – - Runkaus basalts
  - × - Mafic sills & dikes
- ■ Peräpohja, 2.1 Ga Jouttiaapa high Ti -basalt averages (Kyläkoski 2007)
- – Hyrynsalmi, 2.2 Ga GWA-intrusives and later diabases (Kontinen 1987)
- ✱ Kuhmo, Arola pyroxenites (Papunen et al. 2009)
- + Kuhmo, 2.2 Ga pyroxenite dikes (Papunen et al. 2009)
- + Kuhmo, 2.2 Ga wehrlite dikes (Papunen et al. 2009)
- – Koli, 2.2 Ga layer sill profile (Pekkarinen et al. 2006)
- ● Koli, 2.1 Ga T1 Fe-tholeiites (Pekkarinen et al. 2006)
- ● Koli, 1.97 Ga T2-tholeiites (Pekkarinen et al. 2006)
- ■ Karelian province, miscellaneous mafics & ultramafics:
  - ▲ - Koli-Kaltimo, 2.1 Ga Fe-tholeiite average (Vuollo et al. 1992)
  - ▲ - Koli-Kaltimo, 1.97 Ga tholeiite average (Vuollo et al. 1992)
  - – - Peräpohja, 1.98 Ga amphibolites (Hanski et al. 2005)
- ○ Kola, Pechenga series 2.05-1.98 Ga mafic volcanics (Hanski 1992)
- ● Jormua, 1.95 Ga main suite lavas & dykes (Peltonen et al. 1996)
- ■ Outokumpu-Jormua metasomatic ultramafic averages (Kontinen et al. 2006)
- ▲ Outokumpu-Vuonos metaperidotite average (Kontinen et al. 2006)

Weathered mafics–ultramafics, paleosols & sediments:

- ■ Hekpoort, 2.22 Ga basaltic andesite averages (Oberholzer & Eriksson 2000)
- ◆ Hekpoort, 2.2 Ga Gaborone paleosol Strata 1. (Yang & Holland 2003)
- △ Schreiber Beach, 1.9 Ga basaltic paleosol profile (Frei & Polat 2013)
- ▲ Hainan, fresh Neogene basalt (Ma et al. 2007)
- ▲ Hainan, weathered Neogene basalt (Ma et al. 2007)
- ● Gebel Hamza, Lower Miocene smectitic clay (Abayazeed 2012)
- ● Fayum, Upper Eocene smectitic clay (Abayazeed 2012)
- ▲ Lomie ultramafics & weathering products (Ndjigui et al. 2008)

Metalliferous marine sediments:

- △ Tyrrhenian Sea, Eolo seamount metalliferous sediments (Dekov et al. 2009)
- ◆ MAR, Lucky Strike metalliferous sediments (Dias et al. 2008)

FIG. 8. a) Ti–Zr–Al -ratio diagram[2] for GTK samples showing the mafic component in TV fm mudstones–siltstones. Fennoscandian and global reference lithologies are plotted for comparison. *(Literature references are given only here, but are fully listed in Laitala 2014a).* **b)** Insert diagram shows all GTK analyses with legends.

[2] *Diagram adopted from Fralick, P. 2003. Geochemistry of clastic sedimentary rocks: ratio techniques. In: Lentz, D.R. (ed.) Geochemistry of Sediments and Sedimentary Rocks: Evolutionary Considerations to Mineral Deposit-Forming Environments. Geological Association of Canada, GeoText 4, p. 85–103.*

siliciclastic intertidal flat (Laitala 2014b; see e.g. Tice and Lowe 2006; Schopf 2012). Dynamic, rapid deposition also for the metal-rich muds can be inferred from relatively thick, graded-laminated to bedded Mn- and pyrrhotite-rich muds in pictures 436.72–436.37.

The pyritiferous mudstone member of TV fm displays overall similar sedimentary features as the pyrrhotitic mudstone mbr, but gradually introduces pyrite as an increasing diagenetic and syngenetic sedimentary component (426.60–402.03). Laminated pyrrhotite-rich lithologies in 417.92 possibly features a four-element rythmite consisting of flood–ebb–flood–ebb -laminae (Archer 1998) representing one day, or mere semidiurnal ebb-tide couplets representing deposition during two days of the spring-tide maxima. Silt-laminated pyritiferous mudstones in 408.90–407.73 may display seasonal variations in coarser sediment influx (combined with weak tidal signatures), and sandy sequence in 407.73 may represent a graded mass-flow bed, or gradually waning river-fed flood-plume sedimentation. Virtasalo et al. (2014) have obtained marine isotopic signatures from high-resolution isotopic studies of pyrite-rich laminites at 406.55–406.15.

Thinly- to microlaminated, partly biomat-like regular pyritic shales (160.43, TS 67.20) of lithologically distinctive Kuikkalampi fm resemble much of those described by Schieber (1989), and KU fm may represent a coeval distal deep-water facies to TV fm, or later sedimentation.

Geochemistry. Geochemical results of this GTK study are discussed here only briefly, being exemplified in Figs. 5., 7. and 8. Overall, Ni-Zn-Cu-(Co-Mo) correlate well in TV fm and follow the increase of black, clay-rich sapropel mud component. Scatter in Ni/TOC may partly result from particular carbonaceous matter sedimenting also as silt-size and larger detrital grains. The observed metal trends agree with paleomarine redox-controlled processes (e.g. Leventhal 1998). Manganiferous mudstone lithologies may indicate proximity to nearby fault-sourced brine fluids (Large et al. 1998) or volcanic hydrothermal complexes (Lydon et al. 2000), but are also a feature of shallow environments in redox-stratified marine basins (Force and Cannon 1988; see also Berner 1981). As the formation of sedimentary pyrite is closely dependent on the availability of reactive organic carbon (Berner 1982), dissolved or nanoparticulate iron (Raiswell and Canfield 2012) and bacterially reducible sulfate, our chemical data implies an environment where all of these above mentioned conditions are met.

Results: Interpreting the Provenance and Environment

Talvivaara fm metalliferous mudstones – evidence for supracrustal weathering and mafic clays. Fig. 8. shows Ti-Zr-Al –diagram for Talvivaara samples (GTK) examined in this study. A comparison with global and Fennoscandian literature data shows that TV fm samples plot distinctly towards mafic–ultramafic sources. This is compatible with Lahtinen et al. (2010), who identified a significant component originating from ca. 2.1 Ga continental basalts in Finnish Lower Kaleva (Ludicovian) sediments. We interpret that Fig. 8. necessitates a genetic model for the metal-enrichment in Talvivaara formation that is related to the primary composition and properties of the sedimentary particles, not random external factors. High levels of preserved C_{org} in the Talvivaara samples indicates also exceedingly high primary productivity, which would correspondingly require practically unlimited nutrient supply. A cyanobacterial, bacterial, and archaeal origin for the biomass is here presumed. Phosphorus is one essential rate-limiting nutrient for photosynthetic primary producers, and riverine delivery from oxidatively weathered continental lithologies provides the largest flux of PO_4^{3-} to the oceans (Papineau 2010; Van Kranendonk et al. 2012). Basaltic rocks have high P -contents, and fine clay-rich basaltic soils (with adsorbed PO_4^{3-}) are transported especially during flood events: estuaries may serve as short-term repositories for basaltic clays, which are further preferentially exported and hydrodynamically concentrated into nearby offshore zone (McCullogh et al. 2003; Webster et al. 2003; Douglas et al. 2005). In our Talvivaara data, we are seeing features of Fe-Ti -rich smectitic protolith-clay component derived from continental basalts, which could relate to enhanced preservation of organic carbon and metal sequestration in the TV fm sediments (Kennedy 2002; Ossa Ossa et al. 2013). Overall, we find support for a near-estuarine paleoenvironment (Lahtinen 2000), and deep-water tidal rhythmite signatures in Talvivaara fm point towards a dynamical, complexely reprocessed proximal source for the mud–silt -dominated sediments (e.g. Jaeger and Nittrouer 1995: Dalrymple and Choi 2007). Iron appears to have been an unlimiting chemical reagent during the deposition of Talvivaara fm, which likely indicates both abundant detrital contribution (Krapez et al. 2003; Fralick and Pufahl 2006; Kyläkoski et al. 2013) and ferruginous deeper water marine background conditions (Poulton and Canfield 2011), possibly also locally contributed by continental run-off (Schieber 1987).

Conclusions

Conclusions. The preliminary results from our studies of the Paleoproterozoic Talvivaara fm (2.1–2.0 Ga) in Sotkamo, Finland, call for revising the current hydrothermal ore-genetic model for the Talvivaara Ni-Zn-Cu-Co –deposit. Our chemical data and sedimentological interpretations point coherently toward paleoenvironmental, exogenic surficial and redox-processes in concentrating the metals in marine, tidally-dominated deep-water depositional environment. We interpret that the enrichment and sequestration of Ni-Zn-Cu-Co-(Mo-V-U) in the C_{org}- and iron sulfide-rich Talvivaara fm muds is fundamentally linked to major changes in the Earth’s atmospheric and surface environment, as reviewed by Holland (2005). We identify the metal-enriched TV fm as having a distinct protolith-clay component derived from subaerial oxidative weathering of mafic–ultramafic continental lithologies. While our current data does not trace the ultimate sources of local marine sulfur, our resedimented paleoestuarine model for the Talvivaara fm would be consistent with elevated sulfate concentrations by nearby riverine delivery. Sulfate in the global seawater is mostly supplied by oxidative weathering of continental sulfides (e.g. Lyons et al. 2006; Farquhar et al. 2010), and we hypothesize that Talvivaara fm was sedimented near such delivery point. This scenario would also be consistent with the ca. 2.02 Ga emergence of sediment-hosted metal deposits in stratified, shallow basins with oxygenated sulfate-rich surface waters (Leach et al. 2010, p. 602). Semidiurnal tidal rhythmites in TV fm imply unrestricted connection to the global paleo-ocean, but we propose regionally, perhaps temporally, elevated metal concentrations in a narrow seaway situated near Karelian craton-margin.

References

Adkins, R.M. and Eriksson, K.E. 1998. Rhythmic sedimentation in a mid-Pennsylvanian delta-front succession, Magoffin Member (Four Corners Formation, Breathitt Group), eastern Kentucky: a near-complete record of daily, semi-monthly, and monthly tidal periodicities. In: Alexander, C.R. et al. (eds.) Tidalites: Processes and Products. SEPM Spec. Publ. 61, p. 85–94.
Allison, M.A., Nittrouer, C.A. and Kineke, G.C. 1995. Seasonal sediment storage on mudflats adjacent to the Amazon River. Marine Geology 125, 303–328.
Archer, A.W. 1998. Hierarchy of controls on cyclic rhythmite deposition: Carboniferous basins of Eastern and Mid-Continental U.S.A. In: Alexander, C.R. et al. (eds.) Tidalites: Processes and Products. SEPM Spec. Publ. 61, p. 59–68.
Bekker, A., Slack, J.F., Planavsky, N., Krapez, B., Hofmann, A., Konhauser, K.O. and Rouxel, O.J. 2010. Iron formation: The sedimentary product of a complex interplay among mantle, tectonic, oceanic, and biospheric processes. Economic Geology 105, 467–508.
Berner, R.A. 1981. A new geochemical classification of sedimentary environments. Journal of Sedimentary Petrology 51, 359–365.
Berner, R.A. 1982. Burial of organic carbon and pyrite sulfur in the modern ocean: its geochemical and environmental significance. American Journal of Science 282, 451–473.
Cowan, E.A., Cai, J., Powell, R.D., Seramur, K.C. and Spurgeon, V.L. 1998. Modern tidal rhythmites deposited in a deep–water estuary. Geo-Marine Letters 18, 40–48.
Dalrymple, R.W. and Choi, K. 2007. Morphologic and facies trends through the fluvial–marine transition in tide-dominated depositional systems: A schematic framework for environmental and sequence-stratigraphic interpretation. Earth-Science Reviews 81, 135–174.
De Boer, P.L., Oost, A.P. and Visser, M.J. 1989. The diurnal inequality of the tide as a parameter for recognizing tidal influences. Journal of Sedimentary Petrology 59, 912–921.
Douglas, G., Ford, P., Palmer, M., Noble, R. and Packett, R. 2005. Identification of Sediment Sources in the Fitzroy River Basin and Estuary, Queensland, Australia. Cooperative Research Centre for Coastal Zone, Estuary and Waterway Management, Technical Report 13. 32 p.
Farquhar, J., Wu, N., Canfield, D.E. and Oduro, H. 2010. Connections between sulfur cycle evolution, sulfur isotopes, sediments, and base metal sulfide deposits. Economic Geology 105, 509–533.
Force, E.R. and Cannon, W.F. 1988. Depositional model for shallow-marine manganese deposits around black shale basins. Economic Geology 83, 93–117.
Fralick, P. and Pufahl, P.K. 2006. Iron formation in Neoarchean deltaic successions and the microbially mediated deposition of transgressive systems tracts. Journal of Sedimentary Research 76, 1057–1066.
Gehör, S. and Havola, M. 1988. The depositional environment of the early Proterozoic Tuomivaara Iron-Formation and associated metasediments, eastern Finland. In: Laajoki, K. and Paakkola, J. (eds.) Sedimentology of the Precambrian Formations in Eastern and Northern Finland. Geological Survey of Finland, Spec. Pap. 5, p. 109–133.
Goodfellow, W.D. and Lydon, J.E. 2007. Sedimentary exhalative (SEDEX) deposits. In: Goodfellow, W.D. (ed.) Mineral Deposits of Canada: A Synthesis of Major Deposit Types, District Metallogeny, the Evolution of Geological Provinces, and Exploration Methods. Geol. Assoc. of Canada, Mineral Deposits Div. Spec. Publ. 5, p. 163–183.
Hanski, E.J. and Melezhik, V.A. 2013. 3.2 Litho- and chronostratigraphy of the Palaeoproterozoic Karelian formations. In: Melezhik, V.A. et al. (eds.) Reading the Archive of Earth’s Oxygenation. Vol. 1: The Palaeoproterozoic of Fennoscandia as Context for the Fennoscandian Arctic Russia – Drilling Early Earth Project. Springer, p. 39–110.
Holland, H.D. 2005. 100th Anniversary special paper: Sedimentary mineral deposits and the evolution of Earth’s near-surface environments. Economic Geology 100, 1489–1509.
Jaeger, J.M. and Nittrouer, C.A. 1995. Tidal controls on the formation of fine-scale sedimentary strata near the Amazon river mouth. Marine Geology 125, 259–281.
James, H.L. 1966. Chemistry of the Iron-Rich Sedimentary Rocks. U.S. Geological Survey Prof. Pap. 440–W. 61 p.
Jowitt, S.M. and Keays, R.R. 2011. Shale-hosted Ni–(Cu–PGE) mineralisation: a global overview. Applied Earth Science, Transactions of the Institution of Mining & Metallurgy B, v. 120, 187–197.
Karhu, J.A. 1993. Paleoproterozoic evolution of the carbon isotope ratios of sedimentary carbonates in the Fennoscandian Shield. Geological Survey of Finland, Bulletin 371. Geologian tutkimuskeskus, Espoo. 87 p.
Karhu, J.A. and Holland, H.D. 1996. Carbon isotopes and the rise of atmospheric oxygen. Geology 24, 867–870.
Kärki, A. 1988. Stratigraphy of the Kainuu Schist Belt and palaeosedimentology of its Kalevian metasediments at Melalahti, northern Finland. In: Laajoki, K. and Paakkola, J. (eds.) Sedimentology of the Precambrian formations in eastern and northern Finland. Geological Survey of Finland, Special Paper 5, p. 149–164.
Kennedy, M.J., Pevear, D.R. and Hill, R.J. 2002. Mineral surface control of organic carbon in black shale. Science 295, 657–660.
Kontinen, A. 2012. F029 Talvivaara Ni-Zn-Cu. In: Eilu, P. (ed.) Mineral Deposits and Metallogeny of Fennoscandia. Geological Survey of Finland, Spec. Pap. 53, p. 276–280.
Kontinen, A., Peltonen, P. and Huhma, H. 2006. Description and Genetic Modelling of the Outokumpu-type Rock Assemblage and Associated Sulphide Deposits. Final Technical Report for GEOMEX. Geological Survey of Finland, Report M 10.4/2006/1. 378 p.
Kontinen, A., Käpyaho, A., Huhma, H., Karhu, J., Matukov, D.I., Larionov, A. and Sergeev, S.A. 2007. Nurmes paragneisses in eastern Finland, Karelian craton: Provenance, tectonic setting and implications for Neoarchean crustal correlation. Precambrian Research 152, 119–148.
Kontinen, A., Sorjonen-Ward, P., Huhma, H. and Lahtinen, H. 2013. Lithostratigraphy, sedimentary environment and origin of the Talvivaara black schist hosted Ni-Zn-Cu-Co deposit. In: Hölttä, P. (ed.) Current Research: GTK Mineral Potential Workshop, Kuopio, May 2012. Geological Survey of Finland Rep. of Invest. 198, p. 84–90.
Korja, A., Lahtinen, R., Heikkinen, P., Kukkonen, I.T. and FIRE Working Group 2006. A Geological interpretation of the upper crust along FIRE 1. In: Kukkonen, I.T. and Lahtinen, R. (eds.) Finnish Reflection Experiment FIRE 2001–2005. Geological Survey of Finland, Spec. Pap. 43, p. 45–76.
Krapez, B., Barley, M.E. and Pickard, A.L. 2003. Hydrothermal and resedimented origins of the precursor sediments to banded iron formation: sedimentological evidence from the Early Palaeoproterozoic Brockman Supersequence of Western Australia. Sedimentology 50, 979–1011.
Kuehl, S.E., Nittrouer, C.A. and DeMaster, D.J. 1988. Microfabric study of fine-grained sediments: observations from the Amazon subaqueous delta. Journal of Sedimentary Petrology 58, 12–23.
Kvale, E.P. 2012. Tidal constituents of modern and ancient tidal rhythmites: criteria for recognition and analysis. In: Davis, R.A., Jr., and Dalrymple, R.W. (eds.) Principles of Tidal Sedimentology. Springer, p. 1–17.
Kyläkoski, M., Hanski, E. and Huhma, H. 2012. The Petäjäskoski Formation, a new lithostratigraphic unit in the Paleoproterozoic Peräpohja Belt, northen Finland. Bulletin of the Geological Society of Finland 84, 85–120.
Laajoki, K. 2005. Karelian supracrustal rocks. In: Lehtinen, M. et al. (eds.) Precambrian Geology of Finland – Key to the Evolution of the Fennoscandian Shield. Developments in Precambrian Geology 14. Elsevier, p. 279–342.
Laajoki, K. and Saikkonen, R. 1977. On the geology and geochemistry of the Precambrian iron formations in Väyrylänkylä, South Puolanka area, Finland. Geological Survey of Finland, Bulletin 292. 137 p.
Lahtinen, R. 2000. Archaean–Proterozoic transition: geochemistry, provenance and tectonic setting of metasedimentary rocks in central Fennoscandian Shield, Finland. Precambrian Research 104, 147–174.
Lahtinen, R., Garde, A.A. and Melezhik, V.A. 2008. Paleoproterozoic evolution of Fennoscandia and Greenland. Episodes 31, 20–28.
Lahtinen, R., Huhma, H., Kontinen, A., Kohonen, J. and Sorjonen-Ward, P. 2010. New constraints for the source characteristics, deposition and age of the 2.1–1.9 Ga metasedimentary cover at the western margin of the Karelian Province. Precambrian Research 176, 77–93.
Laitala, J.J. 2014a. Petrography, geochemistry and paleosedimentology of sulfidic sedimentary rocks in drill core DDKS-010, Talvivaara ore deposit, Sotkamo, Finland. Department of Geosciences and Geography, University of Helsinki. xxx p. (Unpubl. M.Sc. thesis in English, *in preparation*)
Laitala, J.J. 2014b. Semidiurnal rhythmites, intertidal microbial mat detritus, pyrite beds and thick fluid-mud layers: dynamic subtidal nearshore deposition of iron sulfide-rich carbonaceous mudstones–siltstones of the Paleoproterozoic Talvivaara formation (2.1–2.0 Ga), Finland. Geological Society of America, Abstracts with Programs 46, No. 6, p. 0. *(accepted)*
Large, R.R., Bull, S.W., Cooke, D.R. and McGoldrick, P.J. 1998. A genetic model for the HYC deposit, Australia: Based on regional sedimentology, geochemistry and sulfide-sediment relationships. Economic Geology 93, 1345–1368.
Leach, D.L., Bradley, D.C., Huston, D., Pisarevsky, S.A., Taylor, R.D. and Gardoll, S.J. 2010. Sediment-hosted lead-zinc deposits in earth history. Economic Geology 105, 593–625.
Lecomte, A. et al. *(7 other authors)* 2014. Uraniferous bitumen nodules in the Talvivaara Ni-Zn-Cu-Co deposit (Finland): influence of metamorphism on uranium mineralization in black shales. Mineralium Deposita 49, 513–533.
Leventhal, J.S. 1998. Metal-rich black shales: formation, economic geology and environmental considerations. In: Schieber, J.S., Zimmerle, W. and Sethi, P.S. (eds.) Shales and Mudstones vol. II. E. Schweizerbart’sche Verlagsbuchhandlung, p. 255–282.
Loukola-Ruskeeniemi, K. and Heino, T. 1996. Geochemistry and genesis of the black shale-hosted Ni-Cu-Zn deposit at Talvivaara, Finland. Economic Geology 91, 80–110.
Loukola-Ruskeeniemi, K. and Lahtinen, H. 2013. Multiphase evolution in the black-shale hosted Ni-Cu-Zn-Co deposit at Talvivaara, Finland. Ore Geology Reviews 52, 85–99.
Loukola-Ruskeeniemi, K., Arkimaa, H., Airo, M.-L., Vuoriainen, S., Hyvönen, E., Lerssi, J. and Vanne, J. 2013. Genetic model for the Talvivaara Ni-Cu-Zn-Co deposit and ore potential of black shale units in Finland. In: Jonsson, E. et al. (eds.) Mineral Deposit Research for a High-Tech World. Proceedings of the 12th Biennal SGA Meeting, 12–15 August 2013, Uppsala, Sweden, p. 600–603.
Love, L.G. and Zimmerman, D.O. 1961. Bedded pyrite and micro-organisms from the Mount Isa Shale. Economic Geology 56, 873–896.
Lydon, J.W., Höy, T., Slack, J.F. and Knapp, M.E. (eds.) 2000. The geological environment of the Sullivan Deposit, British Columbia. Geological Association of Canada Mineral Deposits Division Spec. Publ. 1. 834 p.
Lyons, T.W., Gellatly, A.M., McGoldrick, P.J. and Kah, L.C. 2006. Proterozoic sedimentary exhalative (SEDEX) deposits and links to evolving global ocean chemistry. In: Kesler, S.E. and Ohmoto, H. (eds.) Evolution of Early Earth’s Atmosphere, Hydrosphere, and Biosphere – Constraints from Ore Deposits. Geological Society of America Memoir 198, 169–184.
Mackay, D.A. and Dalrymple, R.W. 2011. Dynamic mud deposition in a tidal environment: the record of fluid-mud deposition in the Cretaceous Bluesky Formation, Alberta, Canada. Journal of Sedimentary Research 81, 901–920.
McCulloch, M., Pailles, C., Moody, P. and Martin, C.E. 2003. Tracing the source of sediment and phosphorus into the Great Barrier Reef lagoon. Earth and Planetary Science Letters 210, 249–258.
Melezhik, V.A., Prave, A.R., Hanski, E.J., Fallick, A.E., Lepland, A., Kump, L.R. and Strauss, H. (eds.) 2013. Reading the Archive of Earth’s Oxygenation. Volumes 1–3. Springer, Berlin. 1552 p.
Mudd, G.M. and Jowitt, S.M. 2014. A detailed assessment of global nickel resource trends and endowments. Economic Geology 109, 1813–1841.
Ossa Ossa, F. et al. *(11 other authors)* 2013. Exceptional preservation of expandable clay minerals in the ca. 2.1 Ga black shales of the Francevillian basin, Gabon and its implication for atmospheric oxygen accumulation. Chemical Geology 362, 181–192.
Papineau, D. 2010. Global biogeochemical changes at both ends of the Proterozoic: insights from phosphorites. Astrobiology 10, 165–181.
Pasava, J., Barnes, S.-J. and Vymazalová. 2003. The use of mantle normalization and metal ratios in the identification of the sources of platinum-group elements in various metal-rich black shales. Mineralium Deposita 38, 775–783.
Peltola, E. 1960. On the black schists in the Outokumpu region in eastern Finland. Bulletin de la Commission Géologique de Finlande 192, 1–107.
Potter, P.E., Maynard, J.B. and Depetris, P.J. 2005. Mud and Mudstones: Introduction and Overview. Springer, Berlin. 297 p.
Poulton, S.W. and Canfield, D.E. 2011. Ferruginous conditions: A dominant feature of the ocean through Earth’s history. Elements 7, 107–112.
Raiswell, R. and Canfield, D.E. 2012. The iron biogeochemical cycle past and present. Geochemical Perspectives 1, 1–220.
Rasilainen, K., et al. *(15 other authors)* 2012. Quantitative mineral resource assessment of nickel, copper and cobalt in undiscovered Ni–Cu deposits in Finland. Geological Survey of Finland, Rep. of Inv. 194. 514 p.
Rickard, D. 2012. Sulfidic Sediments and Sedimentary Rocks. Developments in Sedimentology 65, Elsevier, Amsterdam. 801 p.
Riekkola-Vanhanen, M. 2013. Talvivaara mining company – From a project to a mine. Minerals Engineering 48, 2–9.
Schieber, J. 1987. Small scale sedimentary iron deposits in a Mid-Proterozoic basin: viability of iron supply by rivers. In: Appel, P.W.U. and LaBerge, G.L. (eds.) Precambrian Iron Formations. Theophrastus Publ., Athens, p. 267–295.
Schieber, J. 1989. Pyrite mineralization in microbial mats from the mid-Proterozoic Newland Formation, Belt Supergroup, Montana, USA. Sedimentary Geology 64, 79–90.
Schieber, J. 1990. Significance of styles of epicontinental shale sedimentation in the Belt basin, Mid-Proterozoic of Montana, U.S.A. Sedimentary Geology 69, 297–312.
Schopf, J.W. 2012. The fossil record of cyanobacteria. In: Whitton, B.A. (ed.) Ecology of Cyanobacteria II –Their Diversity in Space and Time. Springer, p. 15–36.
Smith, N.D., Phillips, A.C. and Powell, R.D. 1990. Tidal drawdown: a mechanism for producing cyclic sediment laminations in glaciomarine deltas. Geology 18, 10–13.
Talvivaara Mining Co. Plc. 2010. Annual report 2009. Talvivaara Mining Company Plc., Espoo. 134 p.
Talvivaara Mining Co. Plc. 2012. Talvivaara operational and resource update. 28 November, 2012. Talvivaara Mining Company Plc., Stock Exchange Release, 4 p.
Talvivaara Mining Co. Plc. 2014. Annual report 2013. Talvivaara Mining Company Plc., Espoo. 116 p.
Tice, M.M. and Lowe, D.R. 2006. The origin of carbonaceous matter in pre-3.0 Ga greenstone terrains: a review and new evidence from the 3.42 Ga Buck Reef Chert. Earth-Science Reviews 76, 259–300.
Törmälehto, T. 2008. Ore mineralogy and geochemistry of the Kuusilampi deposit, Sotkamo. University of Oulu, Department of Geosciences. 84 p. (Unpubl. M.Sc. thesis, in Finnish)
Törnroos, R. 1982. Sphalerite geobarometry of some metamorphosed sulphide ore deposits in Finland. Geological Survey of Finland, Bulletin 323. 42 p.
U.S. Geological Survey 2013. 2011 Minerals Yearbook: Finland. United States Geological Survey, Minerals Yearbook 2011 [Advance release]. 6 p.
Van Kranendonk, M.J. et al. *(9 other authors)* 2012. A Chronostratigraphic Division of the Precambrian – Possibilities and Challenges. In: Gradstein, F.M. et al. (eds.) The Geologic Time Scale 2012. Elsevier, UK, p. 299–392.
Virtasalo, J.J., Laitala, J., Lahtinen, R. and Whitehouse, M.J. 2014. Microbial mat influence and event deposition of pyritic beds in the Palaeoproterozoic Talvivaara formation. In: Virtasalo, J.J. and Tuusjärvi, M. (eds.) 1st Finnish National Colloquium of Geosciences, Abstract Book, Espoo 19-20 March 2014. Geological Survey of Finland, Guide 58, p. 107–108.
Webster, I.T., Ford, P.W., Robson, B., Margvelashvili, N. and Parslow, J. 2003. Conceptual models of the hydrodynamics, fine sediment dynamics, biogeochemistry and primary production in the Fitzroy Estuary. Cooperative Research Centre for Coastal Zone, Estuary and Waterway Management, Technical Report 8, 43 p.
Williams, G.E. 2000. Geological constraints on the Precambrian history of Earth’s rotation and the Moon’s orbit. Reviews of Geophysics 38, 37–59.
Young, S.A., Loukola-Ruskeeniemi, K. and Pratt, L.M. 2013. Reactions of hydrothermal solutions with organic matter in Paleoproterozoic black shales at Talvivaara, Finland: evidence from multiple sulfur isotopes. Earth and Planetary Science Letters 367, 1–14.

Acknowledgements

The regional specialist, geologist Asko Kontinen (GTK, Kuopio) has essentially laid the foundation for the renewed studies on the sedimentology of the Talvivaara area, and the current work broadly confirms many of his independent observations. We are very grateful for his help, opinions and many discussions during this study. Former chief geologists of the Talvivaara mine Jukka Pitkäjärvi (M.Sc., MAusImm) and Hannu Lahtinen (M.Sc., MAusImm), as well as mining geologist M.Sc. Teemu Törmälehto are thanked for their kind assistance during drill core sampling. Hannu Lahtinen is also warmly thanked for his central role in selecting the optimal core for the GTK studies and for sharing data. Director, Dr. Martin Whitehouse of NordSIM facility, Stockholm, is thanked for contributing to S- and Fe -isotope analyses. We would also like to express our sincere thanks to Prof. Kirsti Loukola-Ruskeeniemi (GTK) for her positive attitude towards this research.